# Preparation and Properties of Cellulose Nanofiber Films with Various Chemical Compositions Impregnated by Ultraviolet-Curable Resin

Bo-Yoen Kim, Song-Yi Han, Chan-Woo Park, Hee-Mun Chae, and Seung-Hwan Lee*

Nanocomposite films were prepared by impregnating cellulose nanofiber (CNF) sheets of various chemical compositions, *i.e.*, lignocellulose nanofiber (LCNF), holocellulose nanofiber (HCNF), and bleached kraft pulp-based nanofiber (BKP-NF), with UV-curable resin. The effects of the CNF sheet porosity on the amount of impregnated resin and the tensile properties of the corresponding nanocomposite films were investigated. The defibration efficiency, viscosity, and filtration time of HCNF and BKP-NF were higher than those of LCNF, and these properties increased with defibration time for BKP-NF. The density and porosity of the LCNF sheets were lower and higher, respectively, than those of the HCNF and BKP-NF sheets. The porosity of the CNF sheets was successfully regulated using organic solvents with different polarities. The impregnated resin amount increased as the CNF sheet porosity and the ratio of monomer to oligomer in the resin increased. The tensile strengths and elastic moduli of all of the nanocomposite films were higher than those of the neat resin films. The specific tensile strength of the nanocomposite decreased with increasing impregnated resin content.

*Keywords: Cellulose nanofiber; Lignocellulose nanofiber; Holocellulose nanofiber; Nanocomposite; UV curable resin; Defibrillation*

*Contact information: College of Forest and Environmental Sciences, Kangwon National University, 1, Gangwondaehak-gil, Chuncheon-si, Gangwon-do, Korea; *Corresponding author: lshyhk@kangwon.ac.kr*

## INTRODUCTION

Cellulose, a straight-chained polysaccharide composed of β-1-4-glucosides, exists in the cell wall of lignocellulosic biomass. During their biosynthesis, cellulose molecules aggregate to form microfibrils *via* the formation of intermolecular and intramolecular hydrogen bonds through hydroxyl groups at the C-2, C-3, and C-6 carbon positions. These microfibrils are known as cellulose nanofibers (CNFs). Cellulose nanofibers are generally classified as microfibrillated cellulose (MFC) or cellulose nanocrystals (CNC) based on the preparation method and the morphological and crystalline characteristics, particularly the aspect ratio and crystallinity. Microfibrillated cellulose has a high aspect ratio and is generally prepared by mechanical fibrillation methods, while CNCs are a rod-shaped product with a somewhat lower aspect ratio, smaller size, and high crystallinity that can be prepared by decomposing the amorphous region of cellulose *via* acid or enzymatic hydrolysis (Habibi *et al*. 2010; Klemm *et al*. 2011; Yu *et al*. 2013).

CNFs have high strength and a low thermal expansion coefficient (Shimazaki *et al*. 2007; Kalia *et al*. 2014) and are therefore promising potential substitutes for glass and synthetic engineering fibers (*e.g.*, aramid fibers) used as reinforcing fillers in composite materials (Lee and Wang 2006; Qua *et al.* 2009; Kalia *et al.* 2011). For example,

Nakagaito and Yano (2008) prepared a nanocomposite composed of MFCs and phenol resin. They reported an elastic modulus of 12 GPa at 40 wt.% MFC content and a thermal expansion coefficient of 10 ppm/K at 60 wt.% MFC, corresponding closely to the values of E-glass. Shibata and Nakai (2010) reported on the mechanical and thermal properties of a nanocomposite prepared by thermosetting a mixture of MFC, epoxy resin, and tannic acid solution. The addition of 10 wt.% MFC resulted in an improvement in tensile strength from 38 MPa for the neat resin to 65 MPa, and as the MFC content increased from 3 to 15 wt.%, the glass transition temperature increased from 76 to 84 °C. Qing *et al.* (2013) reported a tensile strength of 248 MPa and a toughness of 26 $MJ/m^3$ for a CNF-based nanocomposite prepared by impregnating freeze-dried CNF film with 8 wt.% aqueous phenol resin.

Because the diameters of CNFs are smaller than the wavelength of visible light, they suppress light scattering. Therefore, CNFs have attracted significant attention for the preparation of transparent optical materials (Abe *et al.* 2007; Nogi *et al.* 2009). For instance, Jonoobi *et al.* (2014) prepared a nanocomposite film by carrying out a solvent exchange of an MFC hydrogel sheet with acetone, and then impregnating the sheet with cellulose acetate butyrate resin and triethyl citrate as the plasticizer. The resulting nanocomposite with 60 wt.% MFC content showed 60% transparency and a 6.5 GPa elastic modulus.

A coating technique involving the use of an ultraviolet (UV)-curable resin can be employed to protect the material being coated and to improve its physical properties. Because a solvent is not used, the technique is eco-friendly, and the coating can be cured within a period shorter than that required for thermosetting. Therefore, UV-curable resins are attracting attention for their potential applications in various fields. Specifically, acrylic or epoxy resins are used to form a transparent coating layer. Some studies have focused on hybridization using CNFs, which have excellent optical transparency (Iwamoto *et al.* 2007; Okahisa *et al.* 2011).

In general, CNFs from purified cellulose materials have been used as reinforcing filler for nanocomposite preparation. However, there have been few reports on the nanocomposite using lignocellulose nanofibers (LCNF) with three main components of lignocellulose and holocellulose nanofibers (HCNF) with hemicellulose surrounding cellulose. Thus, in this study, three types of CNF nanosheets, *i.e.*, lignocellulose nanofibers (LCNF), holocellulose nanofibers (HCNF), and bleached kraft pulp-based nanofibers (BKP-NF) with various chemical compositions were prepared to impregnate acrylic resins with various molecular weights into the CNF sheets. The CNF sheet porosity was adjusted to vary the amount of resin impregnated into the CNF sheets. The effects on the tensile properties of the nanocomposite were also investigated.

## EXPERIMENTAL

### Materials

*Pinus koraiensis* S. et Z. (40 mesh-sized powder), its holocellulose, and bleached kraft pulp (BKP) samples were obtained from the Kangwon University's Experimental Forest and Moolim P & P (Ulsan, Korea) and used for the preparation of LCNF, HCNF, and BKP-NF, respectively. An emulsion-type polyester acrylate (PA) from BASF (Ludwigshafen, Germany) and 2-hydroxyethyl methacrylate (2-HEMA) from Merck Millipore (Massachusetts, USA) were used as the oligomer and monomer, respectively.

The initiator was 2,4,6-trimethylbenzoyl diphenylphosphine oxide (TPO) from BASF (Ludwigshafen, Germany). Methyl alcohol (MeOH), ethyl alcohol (EtOH), acetone (AC), t-butyl alcohol (t-BuOH), and other chemicals were purchased from commercial sources and used without further purification.

## CNF Preparation

To obtain the holocellulose of *Pinus koraiensis* S. et Z., delignification was conducted as follows. First, 20 g of sample was added to 1200 mL of distilled water containing sodium chlorite (8 g) and acetic acid (1600 µL) and then stirred at 80 °C at a rate of 160 rpm for 1 h. Then, the same amounts of sodium chlorite and acetic acid were added again, and the process was repeated six times for complete delignification. The reactant product was vacuum-filtered and washed with distilled water until a neutral pH was achieved.

Fibrillation for LCNF, HCNF, and BKP-NF was conducted as follows. Aqueous suspensions of 2 wt.% were prepared and stored at 25 °C for 24 h. For defibration, the suspension then underwent a wet disk milling (WDM) process using a disk mill (MKCA6-2, Masuko Sangyo CO., Ltd., Kawaguchi, Japan). The rotation speed was set to 1800 rpm, and the clearance between the two disks was set to 50 to 120 µm.

## Preparation of CNF Sheets and Nanocomposites

A CNF suspension (296 mL) with 0.15 wt.% solid content was prepared and subjected to vacuum filtration by pouring the suspension into a silicone-coated paper filter with the pore size of 2.5 µm (Whatman, Maidstone, UK) with a 75-mm diameter. The filtration time was measured at this stage as a criterion for the degree of defibrillation. Thus-obtained pre-molded gel-like sheets were hot-pressed for 5 min at 105 °C with a pressure of 0.59 MPa. To adjust the density of the sheets, solvent exchange was conducted using organic solvents with different polarities (MeOH, EtOH, AC, and t-BuOH). The filtrated, gel-like sheet was immersed in the solvent for 3 h. This process was repeated four times for complete substitution of water with organic solvent. The obtained sheets were then dried at 30 °C for 24 h.

For nanocomposite preparation, the oligomer/monomer ratios (w/w) were set at 8:2, 7:3, and 6:4, and the UV-curing initiator (5 wt.% in the basis of resin weight) was added. The mixture was stirred at 35 °C in a shaking incubator (VS-101Si, Vision Scientific Co. Ltd., Seoul, Korea) at 200 rpm. Then, the mixture was impregnated into the CNF sheets for 24 h under 0.02 MPa of pressure. The UV curing was performed by using a UV curing apparatus (RX-H1000D, Raynics Co., Gwangmyoung, Korea) equipped with a 1000-W mercury lamp with main wavelengths of 240 to 400 nm. A pure resin sheet was prepared as the control sample.

## Measurements

For the morphological observations of the CNFs, the CNF suspension (0.001 wt.%) was vacuum-filtrated on a membrane filter (PTFE, pore size 0.2 µm, Toyo Roshi Kaisha Ltd., Japan) to obtain a thin film. The water in the film was completely exchanged with t-BuOH, and the film was freeze-dried to protect the aggregation of CNFs. The dried film was subjected to carbon coating (Spin coater, ACE-200, Dong-ah Tech & Trade Corp., Seoul, Korea) and observed using a scanning electron microscope (FE-SEM, S-4800, Hitachi Co. Ltd., Tokyo, Japan) in the Central Laboratory of Kangwon National University.

The viscosity of the CNF suspension (1 wt.%) was measured using a viscometer (Viscometer DV-II+ Pro, Brookfield, MA) equipped with a temperature controller (maintained at 25 °C) with spindle 34. Measurements were repeated three times, and the average value was used. The tensile tests for the samples (5 mm × 0.4 mm × 50 mm) of CNF sheets and nanocomposites were conducted using a tensile strength testing apparatus (GB/H50K, Hounsfield test equipment Ltd., Redhill, UK) with a cross-head speed of 5 mm/min and span length of 30 mm. The density and porosity of the CNF sheets and the impregnated resin content were calculated using the following equations.

$$\textit{Density}\ (\mathrm{g/cm^3}) = \textit{Mass}\ (\mathrm{g}) \,/\, \textit{Volume}\ (\mathrm{cm^3}) \quad (1)$$

$$\textit{Porosity}\ (\%) = (1 - \rho_s / \rho_c) \times 100 \quad (2)$$

where $\rho_s$ is the density of the sheet (g/cm$^3$), $\rho_c$ is the density of cellulose (1.5 g/cm$^3$) (Sehaqui *et al.* 2011), and the volume of the samples was calculated by measuring the dimension of width, length, and thickness,

$$\textit{Impregnated resin content}\ (\%) = (M_2 - M_1) / M_1 \times 100 \quad (3)$$

where $M_1$ is the mass (g) of the CNF sheet, and $M_2$ is the mass (g) of the nanocomposite film.

## RESULTS AND DISCUSSION

Figure 1 shows the morphological characteristics of LCNF, HCNF, and BKP-NF obtained with 10 repeating passes of WDM. The LCNF diameters were greater than those of HCNF and BKP-NF at the same WDM pass. Lignin-like particles and large aggregated fibers appeared in the LCNF, whereas the diameters of HCNF and BKP-NF were evenly distributed at approximately 50 nm. Lignocellulose nanofiber contains hemicellulose and lignin, which adhere to cellulose microfibrils, thus its defibrillation would be more difficult than that of HCNF or BKP-NF. However, the SEM images just show the limited area of the CNFs. Thus, the viscosity and filtration time were measured as an indirect evaluation method of the defibrillation degree.

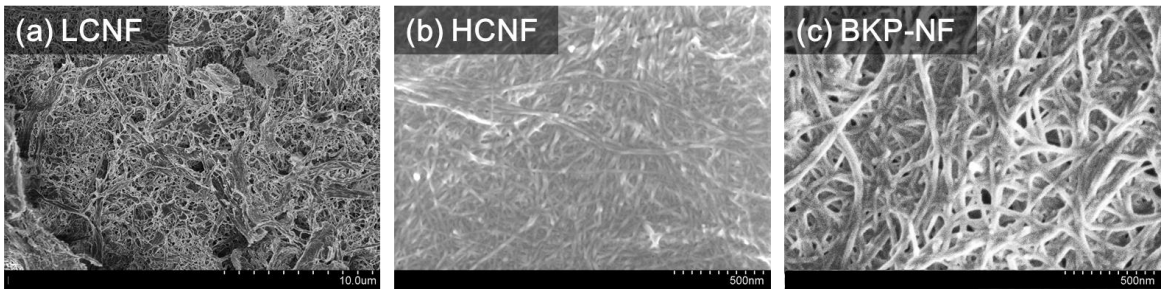


**Fig. 1.** SEM images of nanofibers. Number of WDM passes: 10

Figure 2 shows the viscosity of HCNF and BKP-NF with different numbers of WDM passes. The viscosity of LCNF was too low to measure under the same conditions as HCNF and BKP-NF. The BKP-NF showed a lower viscosity than HCNF, which may have been due to the existence of hemicellulose (Krawczyk *et al.* 2011). In BKP-NF, the viscosity increased as the number of WDM passes was increased, raising the degree of

defibrillation. Ryu *et al.* (2011) investigated the viscosity changes of a CNF suspension according to the number of WDM passes from 1 through 60. They reported that the viscosity increased until 50 passes, and then remained steady because of the increase in the surface area of the CNF with the increasing number of passes.

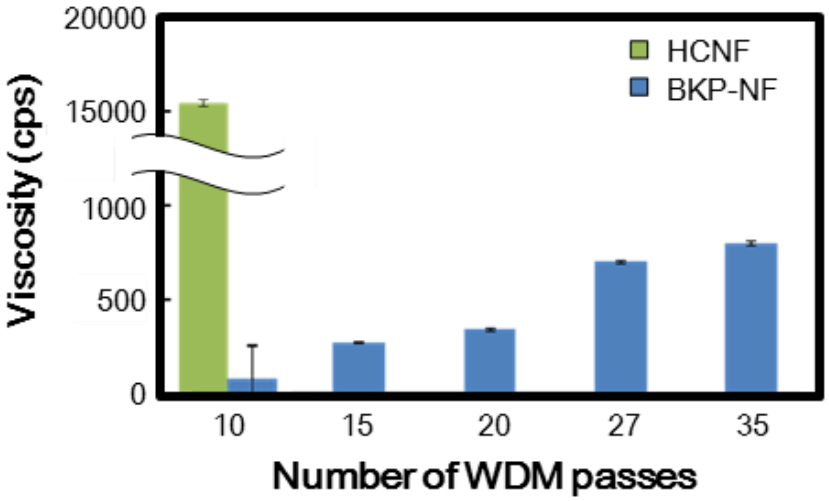


**Fig. 2.** Viscosity of HCNF and BKP-NP with various numbers of WDM passes

Figure 3 shows the filtration time of CNFs prepared with 10 WDM passes and the effect of the number of WDM passes on the filtration time for BKP-NF. Lignocellulose nanofiber showed the shortest filtration time because of the presence of hydrophobic lignin and a low degree of defibrillation. The filtration time of HCNF was 29 h, which was longer than that of BKP-NF. This result is consistent with the fact that the water retention capacity of hemicellulose is greater than that of cellulose (Duchesne *et al.* 2001; Iwamoto *et al.* 2007; Chaker *et al.* 2013). The filtration time increased with the increasing number of WDM passes. This can be considered indirect evidence of the increase in specific surface area with the increase in the number of passes (Chang *et al.* 2012; Jang *et al.* 2012).

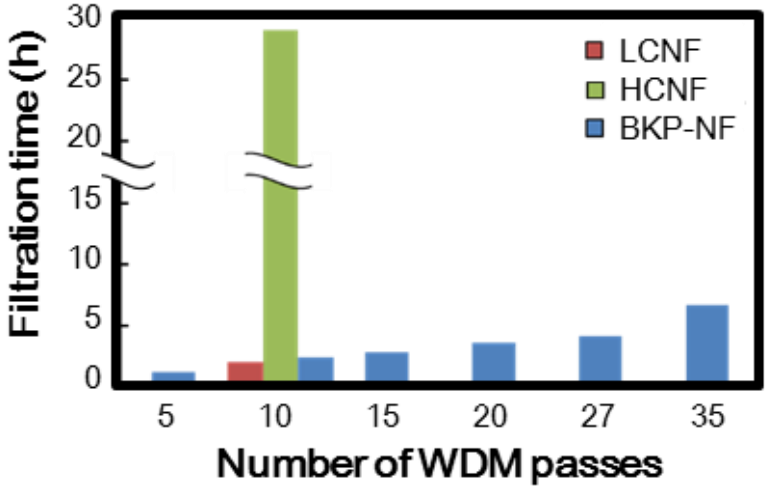


**Fig. 3.** Filtration times for three types of CNFs

Figure 4 shows the density and porosity of CNF sheets and the effect of the number of WDM passes on the density and porosity of BKP-NF sheets. The density and porosity of the LCNF sheet were the lowest and highest, respectively. The density and porosity of the HCNF and BKP-NF sheets were similar at the same number of WDM passes (10 passes). This result is considered to be due to differences in the defibrillation degree and chemical composition. When the number of passes increased, the density and porosity showed increasing and decreasing tendencies, respectively.

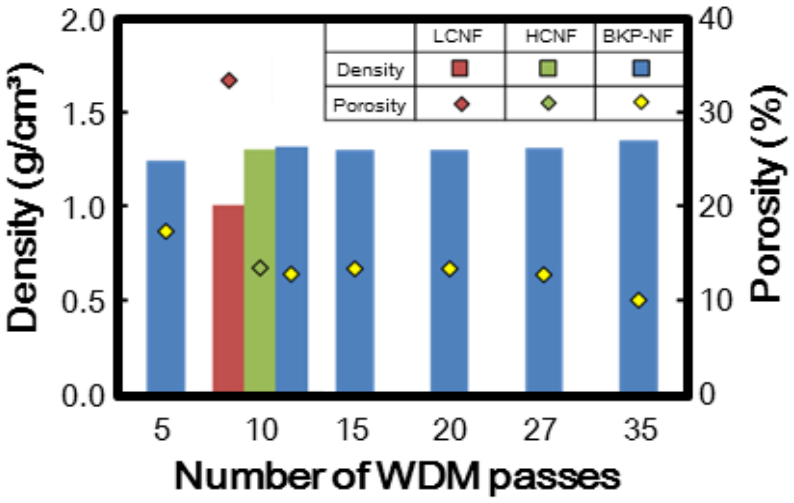


**Fig. 4.** The density and porosity of nanosheets prepared from three CNFs and the effect of the number of WDM passes on the density and porosity of BKP-NF sheets

Figure 5 shows the tensile strength and elastic modulus of nanofiber sheets, neat resin films, and the three CNF-reinforced nanocomposites with various composition ratios of oligomer to monomer. The tensile strengths of the nanosheets manufactured from LCNF, HCNF, and BKP-NF were 18, 97, and 83 MPa, respectively. The tensile strength of the LCNF nanosheet was about 5.5 times lower than those of the other nanosheets. Compared to neat resin films and nanocomposites, LCNF nanosheets showed lower tensile strengths, whereas HCNF and BKP-NF nanosheets showed higher values. Moreover, the tensile strength of the LCNF-based nanocomposite was 35 MPa to 40 MPa, which was lower than those of the other nanocomposites. This may be attributed to the low tensile strength of the LCNF nanosheet itself. However, the tensile strengths of all of the nanocomposite films were higher than those of the neat resin films, for all oligomer/monomer ratios. As the monomer content was increased, the tensile strength of the neat resin film decreased. However, the tensile strength of the nanocomposite film increased with increasing monomer content. This result may be because of the increased fluidity, resulting in an increased amount of impregnated resin in the nanosheet. Liu *et al.* (2013) reported the effect of the amount of impregnated epoxy resin in a regenerated cellulose nanosheet on the tensile strength of the nanocomposite. With an increased amount of impregnated resin, from 5 to 15 wt.%, the tensile strength increased from 93 to 144 MPa, which was higher than that (88 MPa) of the neat epoxy resin film. Similar to the tensile strength, the elastic moduli of all nanocomposites were higher than those of the neat resin films, for all oligomer/monomer ratios. However, the elastic modulus showed a decreasing tendency as the monomer ratio increased.

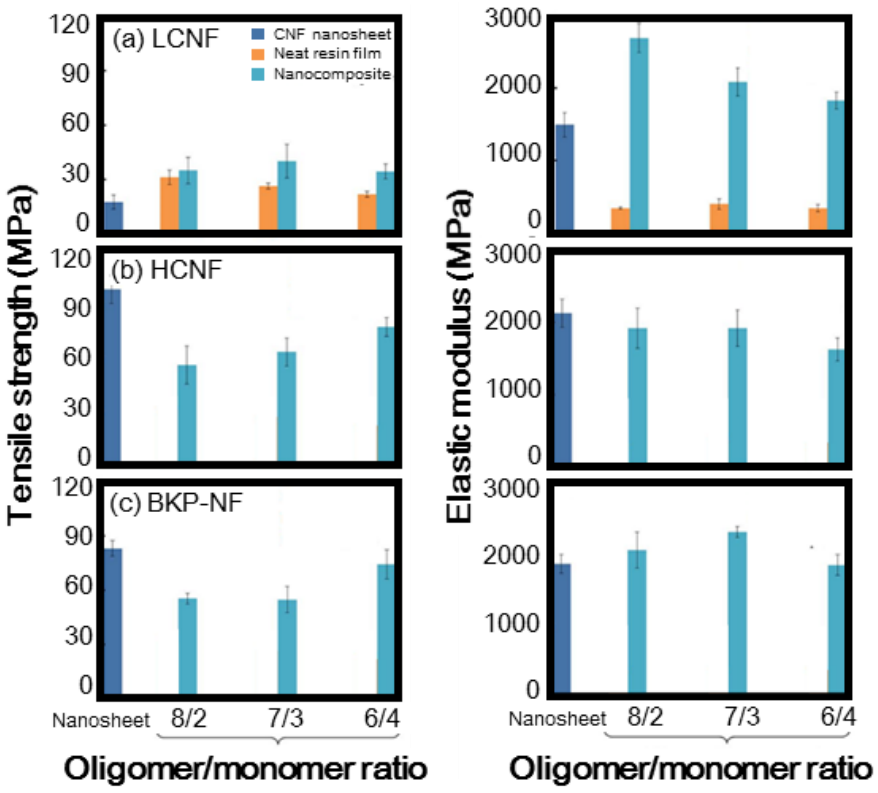


**Fig. 5.** Effect of various oligomer/monomer ratios of UV-curable resin on the tensile strength and elastic modulus of nanocomposite films reinforced with (a) LCNF, (b) HCNF, and (c) BKP-NF

Figure 6 shows the effect of the mechanical defibration level of BKP-NF on the tensile strength and elastic modulus of nanosheets and nanocomposite films with various oligomer/monomer ratios. As the number of WDM passes increased to 20, the tensile strengths and elastic moduli of the nanosheet and all nanocomposite films increased and then decreased. This may be because of the fiber degradation at more than 20 passes. Iwamoto *et al.* (2007) also reported a decreasing tendency in tensile strength and elastic modulus of nanosheets when the number of WDM passes surpassed 15. They explained this phenomenon with the decrease in the degree of polymerization and crystallinity of the cellulose as the number of passes through the grinder increased. The tensile strengths of all of the nanocomposites were lower than those of the nanosheets throughout the entire range of the number of WDM passes, and they increased with the increasing ratio of monomer to oligomer. However, the nanocomposites showed higher elastic moduli values than the nanosheets, and there were no significant differences among the different oligomer/monomer ratios.

To examine the influence of the nanosheet porosity on the impregnation amount of resin, the porosity of the BKP-NF nanosheet (35 WDM passes) was adjusted by solvent exchange of water with solvents of various polarities (MeOH, EtOH, AC, and t-BuOH). As shown in Fig. 7, the porosity increased as the solvent polarity decreased. Specifically, when substituted with AC and t-BuOH, the porosities were 40.00% and 46.67%, respectively, which are high values. This may be because of the lower surface tension of the solvents than water, which could suppress the coagulation of CNFs during the drying of the solvent.

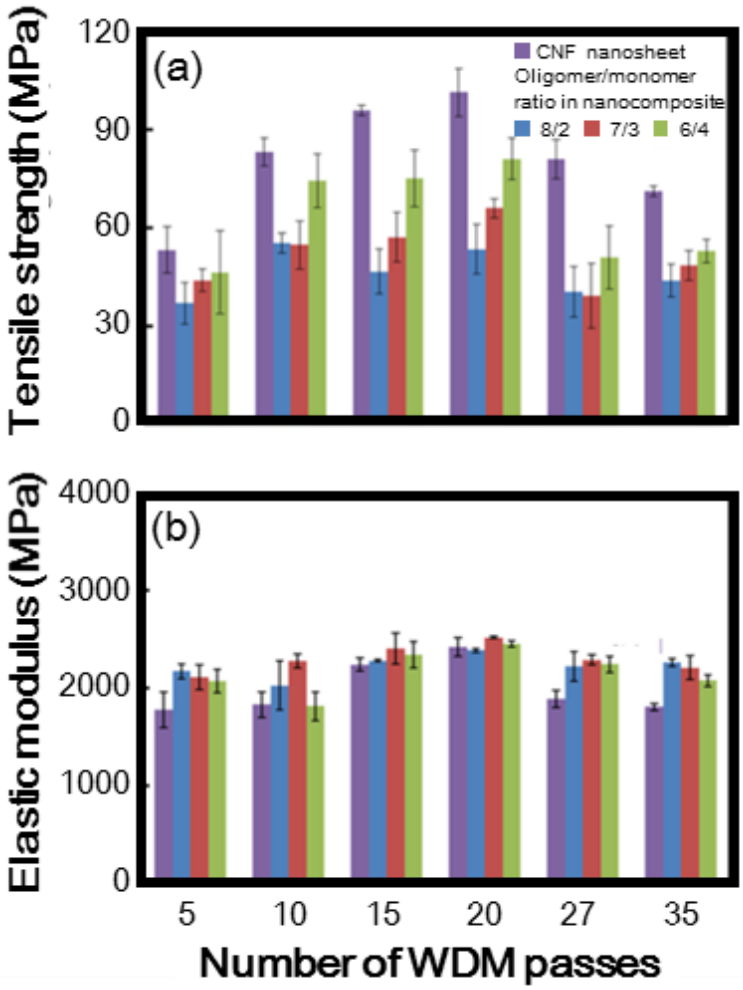


**Fig. 6.** Effect of the number of WDM passes on the (a) tensile strength and (b) elastic modulus of BKP-NF nanosheets and nanocomposite films with various oligomer/monomer ratios

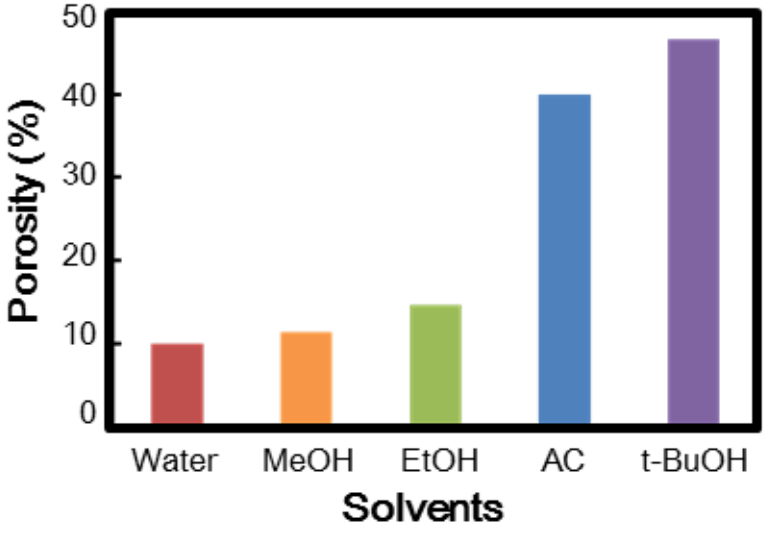


**Fig. 7.** Porosity variation of BKP-NF nanosheets prepared by solvent exchange of water

Figure 8 shows the relationship between the porosity of BKP-NF nanosheets and the impregnated resin content, as well as the relation between specific tensile strength and the impregnated resin content with various oligomer/monomer ratios. The impregnated resin content was closely related to the porosity of the nanosheets, showing an increase in the impregnated resin content with increasing porosity. Furthermore, with increasing monomer ratio, the impregnated resin content also increased. This may be because of the increase of fluidity that occurs with increasing the monomer ratio, as discussed above. The densities of nanocomposites with different impregnated resin contents will differ, which may result in the different tensile strengths. Thus, specific tensile strength was calculated, as shown in Fig. 8. Specific tensile strength decreased with the increasing impregnated resin content for all oligomer/monomer ratios. Nanocomposites with a higher monomer ratio showed higher specific tensile strength. Furthermore, the increase in the impregnated resin content resulted in lower tensile strength, as the tensile strength of the neat resin sheet was lower than that of the nanocomposite, as shown in Fig. 5.

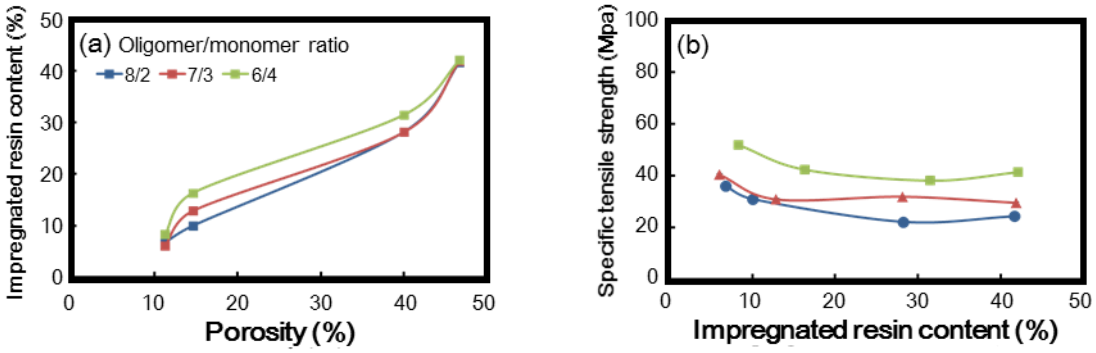


**Fig. 8.** Relationships between (a) the BKP-NF nanosheet porosity and the impregnated resin content and (b) between specific tensile strength and the impregnated resin content with various oligomer/monomer ratios

## CONCLUSIONS

1. The different chemical compositions of three kinds of nanofibrillated cellulose (LCNF, HCNF, and BKP-NF) yielded different defibration degrees, morphological characteristics, and water retention capabilities.
2. Nanopaper sheets were prepared from three CNFs with different characteristics and impregnated by UV-curable resin with different molecular weights to prepare the nanocomposite film. The porosity of the CNF sheets was successfully regulated, affecting the impregnated resin amount. The impregnated resin amount increased as the porosity of the CNF sheet and the ratio of monomer to oligomer in the resin increased.
3. The tensile strengths and elastic moduli of all of the nanocomposite films were higher than those of the neat resin films. Moreover, the specific tensile strength of the nanocomposite showed a decreasing tendency with increasing content of the impregnated resin.
4. The obtained results are expected to provide a positive outlook on the application of CNF and UV-curable resin hybridization in the field of coating.

## ACKNOWLEDGMENTS

This study was carried out with the support of "Forest Science & Technology Projects (Project No. S211316L010120)" provided by Korea Forest Service and Basic Science Research Program through the National Research Foundation of Korea (NRF) funded by the Ministry of Education (No. NRF-2015R1D1A1A01061522).

## REFERENCES CITED

Abe, K., Iwamoto, S., and Yano, H. (2007). "Obtaining cellulose nanofibers with a uniform width of 15 nm from wood," *Biomacromolecules* 8(10), 3276-3278. DOI: 10.1021/bm700624p

Chaker, A., Alila, S., Mutjé, P., Vilar, M. R., and Boufi, S. (2013). "Key role of the hemicellulose content and the cell morphology on the nanofibrillation effectiveness of cellulose pulp," *Cellulose* 20(6), 2863-2875. DOI: 10.1007/s10570-013-0036-y

Chang, F., Lee, S. H., Toba, K., Nagatani, A., and Endo, T. (2012). "Bamboo nanofiber preparation by HCW and grinding treatment and its application for nanocomposite," *Wood Science and Technology* 46(1), 393-403. DOI: 10.1007/s00226-011-0416-0

Duchesne, I., Hult, E. L., Molin, U., Daniel, G., Iversen, T., and Lennholm, H. (2001). "The influence of hemicellulose on fibril aggregation of kraft pulp fibres as revealed by FE-SEM and CP/MAs 13C-NMR," *Cellulose* 8(2), 103-111. DOI: 10.1023/A:1016645809958

Habibi, Y., Lucia, L. A., and Rojas, O. J. (2010). "Cellulose nanocrystals: Chemistry, self-assembly, and applications," *Chemical Reviews* 110(6), 3479-3500. DOI: 10.1021/cr900339w

Iwamoto, S., Nakagaito, A. N., and Yano, H. (2007). "Nano-fibrillation of pulp fibers for the processing of transparent nanocomposites," *Applied Physics A-Materials Science & Processing* 89(2), 461-466. DOI: 10.1007/s00339-007-4175-6

Jang, J. H., Kwon, G. J., Kim, J. H., Kwon, S. M., Yoon, S. L., and Kim, N. H. (2012). "Preparation of cellulose nanofibers from domestic plantation resources," *Journal of the Korean Wood Science and Technology* 40(3), 156-163. DOI: 10.5658/WOOD.2012.40.3.156

Jonoobi, M., Aitomäki, Y., Mathew, A. P., and Oksman, K. (2014). "Thermoplastic polymer impregnation of cellulose nanofibre networks: Morphology, mechanical and optical properties," *Composites Part A: Applied Science and Manufacturing* 58, 30-35. DOI: 10.1016/j.compositesa.2013.11.010

Kalia, S., Dufresne, A., Cherian, B. M., Kaith, B. S., Averous, L., Njuguna, J., and Nassiopoulos, E. (2011). "Cellulose-based bio-and nanocomposites: A review," *International Journal of Polymer Science* 2011, 837875. DOI: 10.1155/2011/837875

Kalia, S., Boufi, S., Celli, A., and Kango, S. (2014). "Nanofibrillated cellulose: Surface modification and potential applications," *Colloid and Polymer Science* 292(1), 5-31. DOI: 10.1007/s00396-013-3112-9

Klemm, D., Kramer, F., Moritz, S., Lindström, T., Ankerfors, M., Gray, D., and Dorris, A. (2011). "Nanocelluloses: A new family of nature-based materials," *Angewandte Chemie International Edition* 50(24), 5438-5466. DOI: 10.1002/anie.201001273

Krawczyk, H., Arkell, A., and Jönsson, A. S. (2011). "Membrane performance during ultrafiltration of a high-viscosity solution containing hemicellulose from wheat bran," *Separation and Purification Technology* 83, 144-150. DOI: 10.1016/j.seppur.2011.09.028

Lee, S. H., and Wang, S. (2006). "Biodegradable polymers/bamboo fiber biocomposite with bio-based coupling agent," *Composites Part A: Applied Science and Manufacturing* 37(1), 80-91. DOI: 10.1016/j.compositesa.2005.04.015

Liu, S., Tao, D., Yu, T., Shu, H., Liu, R., and Liu, X. (2013). "Highly flexible, transparent cellulose composite films used in UV imprint lithography," *Cellulose* 20(2), 907-918. DOI: 10.1007/s10570-013-9877-7

Nakagaito, A. N., and Yano, H. (2008). "The effect of fiber content on the mechanical and thermal expansion properties of biocomposites based on microfibrillated cellulose," *Cellulose* 15(4), 555-559. DOI: 10.1007/s10570-008-9212-x

Nogi, M., Iwamoto, S., Nakagaito, A. N., and Yano, H. (2009). "Optically transparent nanofiber paper," *Advanced Materials* 21(16), 1595-1598. DOI: 10.1002/adma.200803174

Okahisa, Y., Abe, K., Nogi, M., Nakagaito, A. N., Nakatani, T., and Yano, H. (2011). "Effects of delignification in the production of plant-based cellulose nanofibers for optically transparent nanocomposites," *Composites Science and Technology* 71(10), 1342-1347. DOI: 10.1016/j.compscitech.2011.05.006

Qing, Y., Sabo, R., Cai, Z., and Wu, Y. (2013). "Resin impregnation of cellulose nanofibril films facilitated by water swelling," *Cellulose* 20(1), 303-313. DOI: 10.1007/s10570-012-9815-0

Qua, E. H., Hornsby, P. R., Sharma, H. S. S., Lyons, G., and McCall, R. D. (2009). "Preparation and characterization of poly (vinyl alcohol) nanocomposites made from cellulose nanofibers," *Journal of Applied Polymer Science* 113(4), 2238-2247. DOI: 10.1002/app.30116

Ryu, J. H., Youn, H. J., Seo, D. J., Yang, J. Y., and Ryu, J. B. (2011). "Production of nanofibrillated cellulose using grinder and its characterization," in: *Proceedings of the Korea Technical Association of the Pulp and Paper Industry 2011 Conference*, 14-15 April, Gyeongsang National University, Gyeongsangnam-do, Korea, pp. 201-205.

Sehaqui, H., Allais, M., Zhou, Q., and Berglund, L. A. (2011). "Wood cellulose biocomposites with fibrous structures at micro and nanoscale," *Composites Science and Technology* 71(3), 382-387. DOI: 10.1016/j.compscitech.2010.12.007

Shibata, M., and Nakai, K. (2010). "Preparation and properties of biocomposites composed of bio-based epoxy resin, tannic acid, and microfibrillated cellulose," *Polymer Physics* 48(4), 425-433. DOI: 10.1002/polb.21903

Shimazaki, Y., Miyazaki, Y., Takezawa, Y., Nogi, M., Abe, K., Ifuku, S., and Yano, H. (2007). "Excellent thermal conductivity of transparent cellulose nanofiber/epoxy resin nanocomposites," *Biomacromolecules* 8(9), 2976-2978. DOI: 10.1021/bm7004998

Yu, H., Qin, Z., Liang, B., Liu, N., Zhou, Z., and Chen, L. (2013). "Facile extraction of thermally stable cellulose nanocrystals with a high yield of 93% through hydrochloric acid hydrolysis under hydrothermal conditions," *Journal of Materials Chemistry A* 1(12), 3938-3944. DOI: 10.1039/C3TA01150J

Article submitted: July 25, 2016; Peer review completed: October 2, 2016; Revised version received: October 16, 2016; Accepted: October 17, 2016; Published: January 23, 2017.
DOI: 10.15376/biores.12.1.1767-1778